Nanoscale

Surface plasmon enhancement of broadband photoluminescence emission from graphene oxide

Journal:	*Nanoscale*
Manuscript ID:	NR-ART-06-2014-003055.R1
Article Type:	Paper
Date Submitted by the Author:	04-Jul-2014

Complete List of Authors:	Neogi, Arup; University of North Texas, Physics; State Key Laboratory of Electronic Thin Film and Integrated Devices, University of Electronic Science and Technology of China, Karna, Sanjay; University of North Texas, Physics Shah, Rakesh; University of North Texas, Physics Phillipose, Usha; University of North Texas, Physics Perez, Jose; University of North Texas, Physics Shimada, Ryoko; Japan Womens University, Math and Physics Wang, Zhiming; State Key Laboratory of Electronic Thin Film and Integrated Devices, University of Electronic Science and Technology of China,

Nanoscale

RSCPublishing

ARTICLE

Surface plasmon enhancement of broadband photoluminescence emission from graphene oxide

Cite this: DOI: 10.1039/xoxxooooox

A. Neogi[a,b], S. Karna[b], R. Shah[b], U. Phillipose[b], J. Perez[b] and R. Shimada[c] Z. Wang[a]

Received 04th June 2014,
Accepted 00th January 2012

DOI: 10.1039/xoxxooooox

www.rsc.org/

The photoluminescence (PL) emission study of both graphene oxide (GO) and partially-reduced graphene oxide (rGO) have been investigated. It has been observed that the GO has broadband emission from green to near infrared range and upon reduction rGO shows blue PL emission. The broadband PL emission is due to the recombination of electron-hole pair in sp^2 domain embedded within sp^3 matrix. The broadband PL emission also suggests the existence of various sizes of sp^2 domain within the same matrix. Further, PL emission from GO in the presence of Au metal thin film has been investigated. It has been observed that the entire broadband emission from GO in the green to near infrared wavelength region is enhanced significantly at room temperature. The Au-GO interface exhibits surface plasmon resonance in the visible wavelength region and is responsible for over 10 fold enhancement in the photoluminescence at ~2.36 eV. The electrical property measurements on the GO and rGO thin films suggested that the rGO exhibit significantly higher electrical conductivity compared to that of GO thin film. Further, GO thin film exhibit semiconducting behaviour. These properties make the material quite suitable for fabrication of new generation photonic devices.

Introduction

Graphene is a two-dimensional zero band gap material having a hexagonal lattice with sp^2 bonded carbon atoms [1-3]. The optical application of graphene is still limited due to gapless band structure. Recently, various approaches have been employed to open the band gap of graphene in order to fabricate high performance devices. Hydrogenation of graphene was employed for reversible modulation of the electronic properties [4]. But, the process is quite unstable and this makes unsuitable for device fabrication. Graphene oxide (GO), a chemical derivative of graphene, has attracted much attention due to controllable band gap [5]. It is a sp3 hybridized chemical structure with epoxy and hydroxyl functional groups covalently attached on the basal plane, whereas carboxylic and carbonyl functional groups are attached primarily at the sheet edges [6-7]. The band gap in GO can be tuned by controlling degree of these oxygen functionalities (i.e., by varying ratio of sp2 to sp3 hybridized states) [5]. The material exhibit insulating behaviour at full oxidation level, but, it behaves as semiconducting at partial oxidation level. The level of oxygen functionalities can be controlled easily by either varying oxidation parameters or following stepwise reduction of oxygen functionalities. This technique allows controlling of size, shape, and fraction of sp2 domains. Solution phase fabrication technique of GO facilitates thin film deposition on variety of substrates with various sizes and shapes [8].

The optoelectronic property of carbon material having sp^2 and sp3 bonding is determined by the π states of the sp^2 cluster [9-11]. The π and π^* levels of sp^2 domain lie within the bandgap of σ and σ^* states of the sp^3 matrix within GO and are strongly localized [9-11]. The photoluminescence (PL) in the GO system is due to recombination of electron-hole pair in sp^2 domain lie within sp^3 matrix. The presence of sp^2 cluster of different sizes within sp^3 matrix with different concentrations can result in broadband emission from semiconducting GO system. Due to the scattering of the PL by the nanosized cluster of GO in solution or solid phase, the PL emission is rather low compared to conventional semiconductor emitters. Surface plasmons can be coupled to the emitted photon and can be used enhance the light emission by increasing the spontaneous emission rate of material system. [12]. For surface plasmon induced enhancement, the dielectric of the metal should match the emission wavelength. Long range plasmons induced by Au thin film is the most suitable metal for the enhancement of the light emission in the visible wavelength regime (> 500 nm) [12]. Graphene based plasmons has been proposed as a platform for stronger light matter interaction [24,25]. In our current work, we demonstrate the enhancement of broadband emission from semiconductor GO using resonant surface

plasmon induced by a thin gold film. Furthermore the electrical transport property of GO and rGO has been investigated as the conductivity of the optoelectronic graphene based material can be tuned by varying the density of sp^3 disorder cluster within sp^2 hybridized structure [9]. The current results has the potential for a new generation of plasmonic nanophotonic devices.

Material Synthesis

The GO was prepared using modified Hummer's method [13]. According to this method, 1 g of graphite powder was mixed in 23 mL of concentrated H_2SO_4 at room temperature (RT) and then 0.5 g of $NaNO_3$ was added to the mixture. The mixture was cooled down to 0°C, and treated with 3 g of KMnO4. The solution was then maintained at 35-40 °C for half an hour and diluted with 47 ml of DI water. Then, 165 ml of DI water was added further to the mixture along with slow addition of H_2O_2 (30%). The mixture was filtered using filter paper (pore size ~ 40 µm) after repeated washing with HCl (1:10) aqueous solution. The residual acids and salt impurities were removed from the mixture via dialysis for two weeks. The final product was freeze dried. The aqueous dispersion of few layer GO was obtained using horn sonicator for 2 hrs. The unexfoliated GO was removed by centrifugation at 4000 rpm. Homogeneous supernatant was obtained with complete exfoliation of almost all of GO sheets. The solid state GO (SGO) and rGO samples for Raman and electrical measurements were fabricated by drop casting of the uniform dispersion on Si coated with 300 nm of SiO_2 as shown schematically in Figure 1. The samples for optical property measurement were prepared by drop casting of GO dispersion on quartz substrate. This produces layered structure of GO and rGO thin film with normal orthogonal to the substrate. GO thin film was of nearly uniform thickness of 235 nm measured by Zygo New View 7300 profilometer and surface morphological of the structure is shown in the Figure 2.

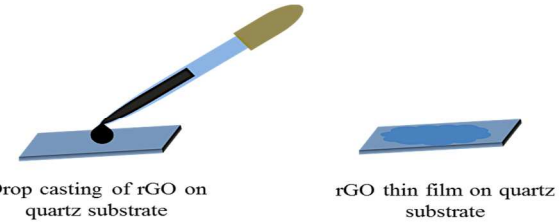

Figure 1 A schematic of drop casting of GO thin film on SiO_2 substrate.

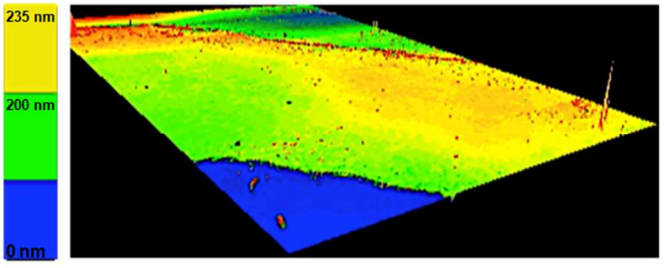

Figure 2: Surface morphology of GO thin film on quartz substrate obtained using profilometer. Substrate is represented by the blue color

Partial reduction of GO (rGO) was obtained chemically using hydrazine monohydrate. For homogenous dispersion of rGO, 1 mg/ml of GO was dispersed in water using ultrasonication. N, N-dimethylformamide (DMF) was then added to the dispersion with volume ratio DMF/water = 9:1 [14] and treated with 50 µl of hydrazine monohydrate. The solution was stirred using teflon coated magnetic stirrer for 5 hrs at a temperature of 65˚C. The rGO sample was purified by repeated filtration and washing with ethanol. Then, the sample was dried in vacuum oven. Black particles in the solution were an indication of slight agglomeration. The agglomerated particles were sonicated for re-dispersion.

Results and discussions

Structural Characterization:

Figure 3 shows transmission electron microscopy (TEM) image of partially reduced GO layers. The figure clearly shows multilayer reduced GO.

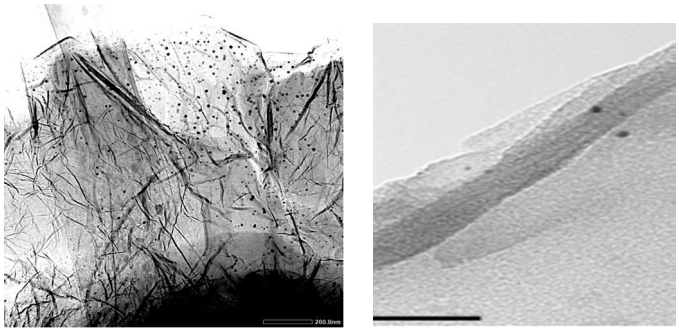

Figure 3: Transmission electron microscopy image of GO. The scale bar represents 100 nm on the right and 200 nm on the left

The structure of the graphine oxide films were further investigated using Raman spectroscopy. The Raman study of GO and rGO thin films deposited on SiO_2 substrate was performed using Almega XR Raman spectrometer with a 532 nm green laser as a source of excitation. Figure 4 shows the normalized Raman spectra of the GO and rGO. The normalization of the peaks was done with respect to the height of G peak. The Raman spectra GO (Figure 4) exhibit a G peak at ~1592 cm-1 that is due to the first order scattering of E2g phonons (in plane optical mode) of sp2 hybridized carbon atoms close to the Γ point [15]. The G peak in GO is shifted from its position in natural graphite (at 1581 cm-1) towards higher frequency due to extensive oxidation. GO also exhibit a D peak at 1350 cm-1 corresponding to defect-induced zone boundary phonons [16].

The Raman spectrum of rGO is shown in Figure 4b. The G and D peaks of rGO appears at 1586 cm-1 and 1355 cm-1,

respectively. This shows that the G peak of rGO shifts towards the position of G peak of graphite that indicates restoration of sp^2 hybridized domains [17]. The integral intensity of G and D peak of GO and rGO was calculated to determine the crystallite size of sp^2 hybridized domains. It has been observed that the crystallite size of sp^2 hybridized domains for GO is ~ 21 nm and the size is reduced to ~17 nm for the case of rGO. The reduction in size of sp^2 hybridized domains is due to chemical treatment with hydrazine monohydrate [15]. Furthermore, the intensity ratio of the D/G peaks in rGO (i.e., ~1.12) was increased compared to that in GO (i.e., ~0.91). This has been attributed to further decreases in the size of in-plane sp^2 hybridized domains due to reduction as we observed from calculation of crystallite size of sp^2 hybridized domains [16]. Further, full width at half maximum (FWHM) of G peaks of GO and rGO are about ~85 cm^{-1} and ~71 cm^{-1}, respectively. This shows that FWHM of rGO is less compared to that of GO and that indicates reduction in disorder on the structure of rGO as compared to that of GO. This reveal that the quantity of sp^2 hybridized domains could be more in rGO compared to that in GO [16].

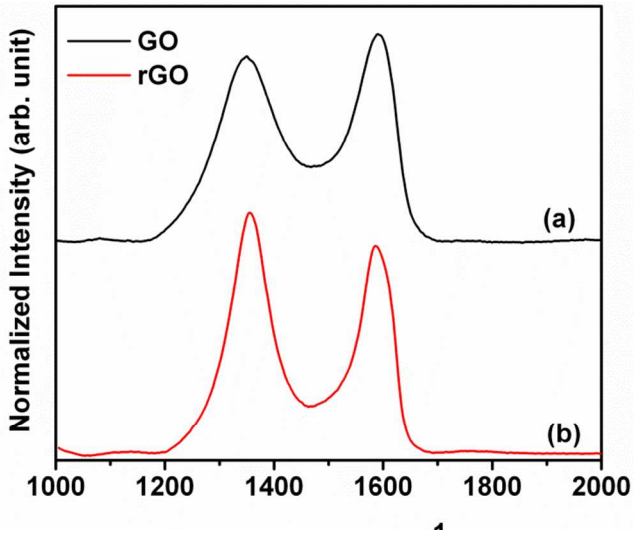

Figure 4 Raman spectra of GO and partially-reduced GO.

Electrical Characterization:

For optoelectronic application of materials, a semiconducting behaviour is desirable in light emitting diodes. The electrical property of GO was analysed using a Semiconductor Device Analyzer (SDA) Agilent Technologies B1500A model. Prior to deposition of GO, the SiO2 substrates were cleaned by sonication in acetone and then an alcohol wash for about 10 minutes followed by a deionized water rinse. Highly doped p-type Si substrates with 100 orientation having oxide thickness of ~285 nm were used. The GO thin film was deposited on the substrate by drop casting method and the sample was dried in vacuum. Initially, a polymer fibre of width ~ 10 µm was placed on the top of GO thin film deposited on the SiO2 substrate. Then, Au (99.99% pure from Alpha Aser) thin film of thickness ~100 nm was thermally deposited using Hind High Vacuum (HHV) auto 306 model. This process was performed at 6×10-6 mbar. The samples were placed "face down" directly above the source of Au specially designed temperature calibrated sample holder. The sample was maintained at a temperature below 50 °C. The polymer fibre was removed after the deposition of Au film using acetone. In this way a thin film strip of GO with Au electrodes on both sides was obtained and used for electrical characterizations.

The IV measurements on the multilayer GO exhibit a Schottky behavior and obey more like a semiconductor bandgap material with low conductivity as shown in Figure 5a. The resistivity of the GO nanostructures was estimated to be ~ 0.0210 Ω-m. However, after chemical reduction of GO, the resistivity of rGO decreases to a value of ~0.0008 Ω-m. At higher applied voltage, the current saturates as shown in Figure 5b. This saturation is presumably due to the electrical reduction of rGO [18,19] induced by the accumulation of excess charge carriers at the metal-semiconductor interface at high-applied voltage. The conductivity of GO and rGO was observed to be in the range of 47.4 Sm-1 and 1238 Sm-1, respectively. The increase in conductivity of rGO is due to reduction in oxygen

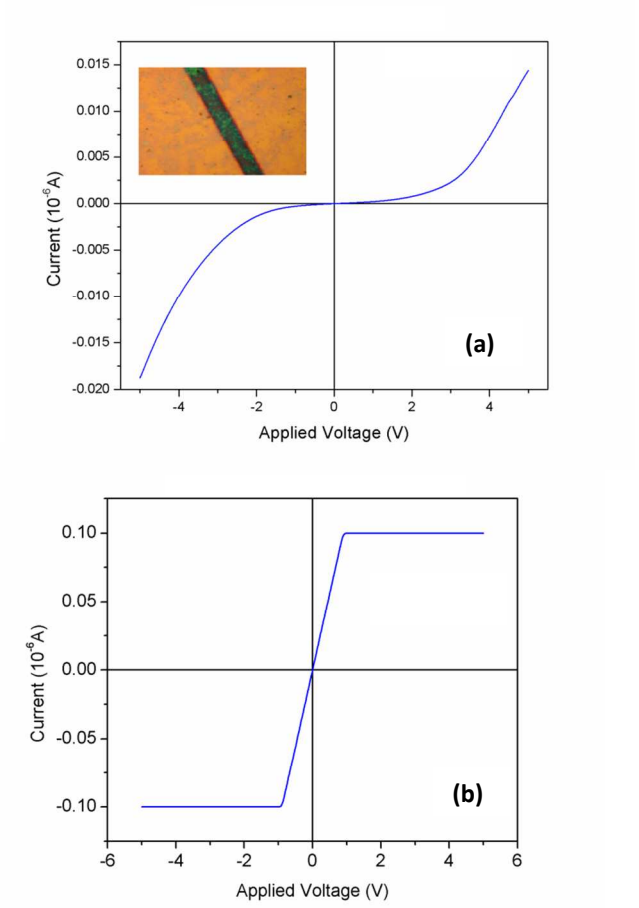

Figure 5: Current voltage characteristics of (a) GO thin film deposited on SiO_2 substrate, and (b) rGO thin film deposited on SiO_2 substrate. The inset shows the device with GO thin film within a channel of width of 10 µm.

functionalities scattering defects sp3 in sp2 structure, which limits the ballistic transport properties [20]. The decreases in sp3 disorder structure in rGO enables higher conductivity that correlates with our Raman analysis.

Optical Characterization:

The semiconducting behavior observed in the electrical transport properties led to the study of the optical properties of the GO and rGO films. The light absorption and emission properties were studied by optical transmission and photoluminescence spectroscopy respectively. Figure 6 shows absorption spectra measure using a spectrophotometer ranging from 180 nm to 1000 nm for GO and rGO solutions within quartz cuvette. The GO exhibit an absorption peak at ~200 nm due to π-π* transitions of C=C hybridized structure. The GO also exhibit a shoulder peak at 240 due to C-C and C=C due to sp2 hybridized structure and another shoulder peak at 303 nm due to n-π* transition of C=O of sp3 hybridized structure [21, 22]. The rGO exhibit an absorption peak at ~260 nm and is due to π-π* transitions of C=C hybridized structure. The peak is red shifted compared to that in GO. The shoulder peaks in the absorption spectrum of rGO are not observed due to the influence of the chemical reduction. This may be due to reduction in the concentration of carboxylic functional groups [22]. Another reason for decrease in the shoulder peak intensity might be due to decrease in intensity ratio of sp^2/sp^3 as observed from the Raman analysis.

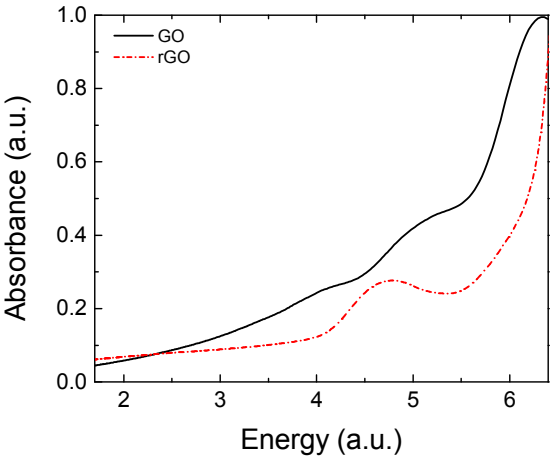

Figure 6: UV-visible absorption spectra of GO and rGO.

PL emission from GO samples in both solution and solid state form was observed at room temperature (RT). The emissions peaks were centred at the blue, and green part of the spectrum with the intensity of the red emission being the weakest. Furthermore, there is not much difference in PL intensities from the solid state and solution phase GO samples. Figure 7 shows optical images of various colors due to PL emissions from GO in aqueous solution phase at a concentration of 0.2 mg/ml excited with a He-Cd laser at wavelength 325 nm. It can be observed from the Figure 7 that the emission consists of various colors red, green and blue comprising of the primary colors for white light spectrum within the same material system. The optical images shown in Figure 7 were collected using various band-pass filters. Figure 7a shows the generation of white light continuum within the cuvette along with the blue light as the bandpass filter between 430-480 nm did not efficiently cut off the other frequencies being generated due to UV excitation.

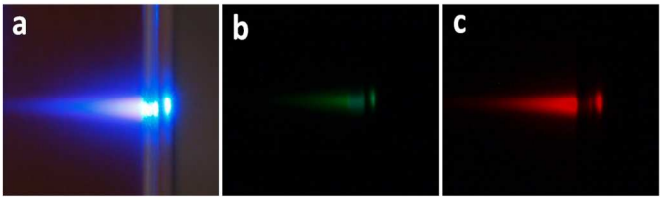

Figure 7 Light emission from aqueous GO solution within a quartz cuvette irradiated by a 442 nm He-Cd laser. (a) Blue emission (b) Green emission (c) Red PL emission.

The PL measurements were carried out using a continuous wave He-Cd laser at operating power of 25 mW at an excitation wavelength 442 nm with Horiba-Jobin Yvon's Triax 320 spectrometer. The blue emission was measured using 325 nm line (10 mW) of the He-Cd laser. The GO thin films were drop casted on a quartz substrate. A part of the substrate was coated with a 30 nm Au film using thermal evaporation. The excitation laser beam spot was expanded to a few mm to take into account any spatial inhomogeneity due to the aggregation of GO thin film on the substrate. The emission from samples under the area of optical excitation was uniformly homogenous.

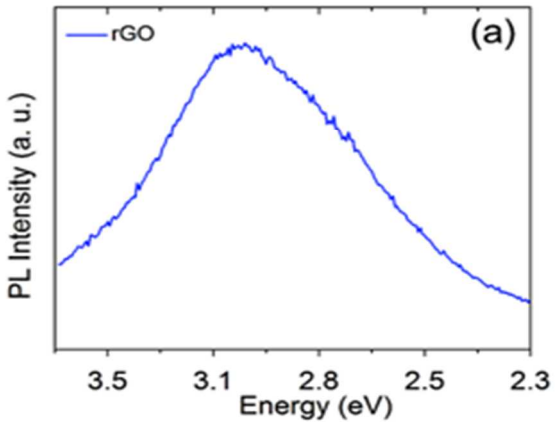

Figure 8a Room temperature PL emission from rGO thin film irradiated with a 325 He-Cd laser

Figure 8a shows the photoluminescence spectrum of partially-reduced GO sample excited at a wavelength 325 nm. PL emission from the r-GO sample with the emission centred in the blue wavelength region at 2.67 eV is observed. The

intensity of the PL emission depends on the concentration of the solution and increases with decreasing concentration. The scattering of the light emitted by the nano-particluates in the solution reduces the emission intensity. The partially reduced GO exhibits less number of disorder induced defect states in between π and π* states and greater number of newly formed cluster like sp2 domain [22]. The electron-hole recombination in these clusters like sp2 domain is responsible for the blue emission [22]. The blue emission from rGO is quite similar to blue emission previous reports [21, 22].

Figure 8b shows PL spectra of GO thin film measured at room temperature. The figure shows the PL emission with peak cantered at 2.36 eV and 2.13 eV. The PL spectra observed from GO is quite similar to the amorphous carbon in which PL emission occurs due to radiative recombination of electron-hole pair in the mid-gap states created by sp2 reach cluster [16, 19]. The energy gap in between the π and π* states depends upon the size of sp2 clusters. There is possibility to have various different sizes of sp2 cluster within the same matrix which could produce PL emissions at broad range [23]. The surface plasmon induced effects of GO thin film was also investigated. For this the GO thin film was partially coated with Au thin films of 30 nm using thermal evaporation at a vacuum level of about 3×10^{-6} Torr. The GO thin films were coated with 30 nm thickness of the Au film with two specific objectives. i) to decouple the surface plasmon modes at the Au-air interface with the SP modes at the GO-Au interface; ii) to minimize the reflection of the generated photoluminescence emission at the 45 °C.[26] A very thin layer of Au film (< 20 nm) would be detrimental to the enhancement as the coupling of the surface plasmon modes at the air-Au interface will interfere with the Au-GO interface and result in increase in non-radiative recombination effects as well as emission in the forward direction. The samples were excited from the substrate side using the 442 nm excitation at an angle of 45 degrees. The PL spectrum was normalized for the reflectivity of the Au thin film using the light reflected from a broadband white light as a baseline. It can be observed from Figure 8b that the PL emission intensity from the Au coated side was enhanced by over 10 folds at 2.36 eV compared to the uncoated section of sample. This enhancement may not be due to increases in reflection from Au thin film as the reflectivity is minimal for the angle at which we have conducted the experiment. The enhancement of similar extent was observed from several spots on the sample. The laser spot size was maintained to be around few mm to avoid any affects of inhomogeneous distribution of the GO films on the substrate. This enhancement of PL emission in the green wavelength is comparable to the enhancement observed in the blue wavelength region from InGaN/Ag plasmonic system. [23] The increase in radiative recombination rate due to the coupling of the PL emission from the GO sheets into the surface plasmon is likely to enhance the emission intensity [27]. The magnitude of enhancement is reduced in the longer wavelength regime where the emission from the GO films is low. The re-absorption of the emitted light by the Au thin film is also likely to play a role in the reduced enhancement of the red or longer wavelength emission.

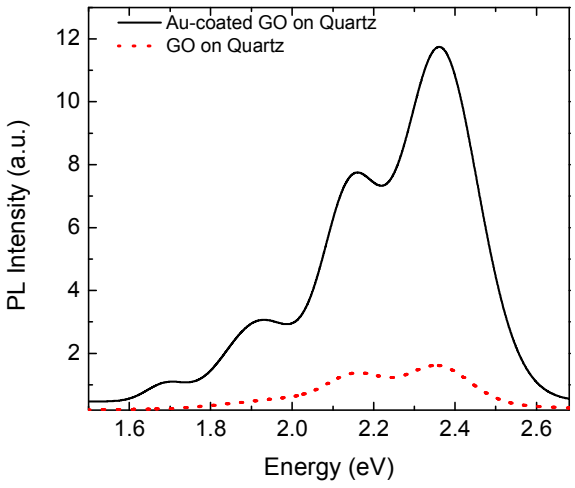

Figure 8b Comparison of room temperature PL emission from GO thin film and the GO thin film with Au metal coating irradiated with 442 nm using He-Cd laser. The figure shows the Au coating enhances PL emission.

Conclusions

The electrical characterization of GO thin film reveal that semiconducting nature of GO with very low conductivity. The conductivity of the material increased significantly by chemical reduction. This implies that the band gap of the material can be tuned by stepwise reduction. The GO thin films exhibit unique broadband well-resolved PL emissions from green to near infrared with relatively less intense blue PL emission whereas rGO exhibit intense blue PL emission. The PL emissions from GO at various energies from visible to near IR region suggest the existence of various sizes of sp^2 rich cluster within same sp3 matrix. The broadband PL emission from GO could be enhanced using the surface plasmons induced by a thin Au film. The enhancement in the green wavelength region where there is serious lack of suitable emitters shows over a 10 fold increase in the light intensity.

Acknowledgements

The authors acknowledge the grant received from the Ministry of Education of the Governments of Chinese under the invitational Foreign Talent Program. A.N. also acknowledges the Faculty Development Research funds from the University of North Texas.

Notes and references

[a] State Key Laboratory of Electronic Thin Film and Integrated Devices, University of Electronic Science and Technology of China, Chengdu 610054, P.R. China
[b] Department of Physics, University of North Texas, P. O. Box 311427, Denton, Texas 76203, USA
[c] Department of Mathematical and Physical Sciences, Japan Women's University, 2-8-1 Mejirodai, Bunkyo-ku, Tokyo, 112-8681, Japan

References:

1. K.S. Novoselov, A. K. Geim, S.V. Morozov, D. Jiang, Y. Zhang, S.V. Dubonos, I.V. Grigorieva, A. A. Firsov, Science, 2004, 306, 666.
2. K. S. Novoselov, A. K. Geim, S. V. Morozov, D. Jiang, M. I. Katsnelson, I. V. Grigorieva, S. V. Dubonos, and A. A. Firsov, Nature, 2005, 438, 197.
3. A.K. Geim, K. S. Novoselov, Nat. Mater., 2007, 6, 183.
4. D. C. Elias, R. R. Nair, T. M. G. Mohiuddin, S. V. Morozov, P. Blake, M. P. Halsall, A. C. Ferrari, D. W. Boukhvalov, M. I. Katsnelson, A. K. Geim and K. S. Novoselov, Nat. Nanotec., 2009, 323, 610-613.
5. Mathkar, D. Tozier, P. Cox, P. Ong, C. Galande, K. Balakrishnan, A. L. M. Reddy, P. M. Ajayan, J. Phys. Chem. Lett., 2012, 3, 986.
6. W. Gao, L. Alemany, L. Ci, P. Ajayan, Nat. Chem., 2009, 1, 403.
7. J. Yan, L. Xian, and M.Y. Chou, Phys. Rev. Lett. 2009, 103, 086802.
8. G. Eda and Manish Chhowalla, Adv. Mater., 2010, 22, 2392.
9. J. Robertson and E. P. O'Reilly, Phys. Rev. B, 1987, 35, 2946.
10. K. P. Loh, Q. Bao, G. Eda and M. Chhowalla, Nat. Chem., 2010, 2, 1015.
11. S. Li Chien, W. Lai, Y. Yeh, H. Chen, I. Chen, L. Chen, K. Chen, T. Nemoto, S. Isoda, M. Chen, T. Fujita, G. Eda, H. Yamaguchi, M. Chhowalla, C. Chen, Angew. Chem. Int. Ed., 2012, 51, 1.
12. J. Lin, A. Mohammadizia, M. Ohtsu, H. Morkoc, A. Neogi, Appl. Phys. Lett., 2012, 97, 221102.
13. W. S. Hummers and R. E. Offeman, J. Am. Chem. Soc., 1958, 80, 1339.
14. S. Park, J. An, I. Jung, R. D. Piner, S. J. An, X. Li, A. Velamakanni, R. S. Ruoff, Nano Lett., 2009, 9, 1593.
15. Zhu, S. Guo, Y. Fang and S. Dong, ACS Nano, 2010, 4, 2429.
16. S. Stankovich, D. A. Dikin, R. D. Piner, K. A. Kohlhaas, A. Kleinhammes, Y. Jia, Y. Wu, S. T. Nguyen, R. S. Ruoff, Carbon, 2007, 45 , 1558.
17. K. N. Kudin, B. Ozbas, H. C. Schniepp, R. K. Prud'homme, I. A. Aksay, R. Car, Nano Lett., 2008, 8, 36.
18. Jung, D. A. Dikin, R. D. Piner, and R. S. Ruoff, Nano Lett. 2008, 8 (12), pp 4283-4287.
19. H. F. Teoh, Y. Tao, E. S. Tok, G. W. Ho and C. H. Sow, Appl. Phys. Lett. 2011, 98, 173105.
20. Y. Chen, B. Zhang, G. Liu, X. Zhuang and E-T. Kang, Chem. Soc. Rev., 2012, 41, 4688.
21. K.S. Subrahmanyam, P. Kumar, A. Nag, C.N.R. Rao, Solid State Commun., 2010, 150, 1774.
22. G. Eda, Y-Y. Lin, C. Mattevi, H. Yamaguchi, H-A. Chen, I-S. Chen, C-W. Chen, M. Chhowalla, Adv. Mater., 2009, 21, 1.
23. K. Okamoto, I. Niki, A. Shvartser, Y. Narukawa, T. Mukai, and A. Scherer, Nat. Materials , 2004, 3, 601.
24. F. H. L. Koppens, D. E. Chang, F. J. G. de Abajo, Nanoletters, 2011, 11, 3370.
25. S. Maier, Nature Physics, 2012, 8, 581.
26. H. R. Gwon and S. H. Lee, Materials Transactions, 2010, 51, 1150.
27. A. Neogi, H. Morkoc, T. Kuroda, A. Tackeuchi, Optics Letters, 2005, 30, 94.

